Mach Reflection Associated with Over-Expanded Nozzle Free Jet Flows

W. L. CHOW*
University of Illinois of Urbana-Champaign, Urbana, Ill.
AND
I. S. CHANG†
Lockheed Missiles and Space Co., Huntsville, Ala.

The occurrence of Mach reflection within the over-expanded nozzle free jet flow has been examined. A flow model emphasizing the interaction between the outer and central core streams has been developed to deal with flow situations where detailed inviscid calculations of the flowfield with Mach reflection are not possible. The results obtained show reasonably good agreement with the available experimental data. This method has also produced comparable results where detailed calculations of the flowfield are possible.

Nomenclature

a, b, c = coefficient defined in text, Eq. (11)
Y_e, R_e = nozzle height or radius at exit
R_o = radius of Mach disk
R = radius
RS = reflected shock
H = height
$X, Y, \bar{Y}$ = coordinates
x_o, y_o = location and height of two-dimensional Mach stem height
P = pressure
M = nozzle Mach number
MS = Mach shock
V_m = maximum flow velocity
V = velocity
σ = wave angle of shock
α = Mach angle
γ = ratio of specific heats
δ = deflection angle of shock
θ = streamline angle

Subscripts

sl = sonic limit
a = ambient or asymptotic state
o = stagnation condition
1 = nozzle flow condition
2 = state behind incident shock
3 = state behind reflected shock at triple point
4 = state behind Mach shock at triple point
b = jet boundary
r = reflected shock
$n3$ = normal reflected shock at triple point
$n4$ = normal Mach shock at triple point
rl = regular reflection limit
MS = Mach shock
T = triple point
$3a$ = fluid states at asymptotic condition above slipline
$4a$ = fluid states at asymptotic condition below slipline
$2_T, 3_T, 4_T$ = states behind incident, reflected, and Mach shock at triple point (axisymmetry flow only)

Received April 12, 1974; revision received August 8, 1974. This work is partially supported by NASA through Research Grant NGL 14-005-140. A major portion of the presented materials is drawn from the Ph.D thesis of the second author.[1]

Index categories: Shock Waves and Detonations; Jets, Wakes, and Viscid-Inviscid Flow Interactions; Supersonic and Hypersonic Flows.

* Professor of Mechanical Engineering. Member AIAA.

† Scientist-Associate-Research; formerly Research Assistant, University of Illinois at Urbana-Champaign, Urbana, Illinois. Member AIAA.

Introduction

FOR nozzles operating under highly over-expanded flow conditions, the shock generated at the edge of the nozzle is so strong that a regular reflection from the centerline is not possible, and the phenomenon of Mach reflection generally appears. Referring to Fig. 1, where an over-expanded two-dimensional nozzle free jet flow is depicted, it may be seen that the occurrence of such a Mach reflection pattern is always manifested by the appearance of a triple point T somewhere along the straight incident shock wave I where a reflected shock R, the Mach shock (or Mach stem) MS, and a slipline SL, indicating the entropy discontinuity, are also originated. Early studies of regular and Mach reflection of shocks within shock tubes by Bleakney and Taub[2] and Polacheck and Seeger[3] established the fact that the inviscid analysis is adequate to study the regular and Mach reflection for shocks of relatively strong strength. However, for fairly weak incident shocks, Mach reflection has been observed when there is no nontrivial solution for the triple point from the inviscid analysis. It may be conceived that under the condition of relatively moderate rate of compression within the shock wave, the subsequent interaction between the flowfield and the shock waves may be such that the viscous effect plays a predominant role in the establishment of the triple point solution. Nevertheless, it is believed that the inviscid triple point solution is still useful in the study of the establishment of the overall free jet flow pattern when Mach reflection occurs, and it is expected to describe the correct trend and behavior of the flow even if the accurate prediction of the flow properties is hampered by the viscous effects such as those prevailing under fairly weak incident shock conditions.

It is thus recognized that the location and the size of the Mach stem occurring within such a free jet flowfield are the

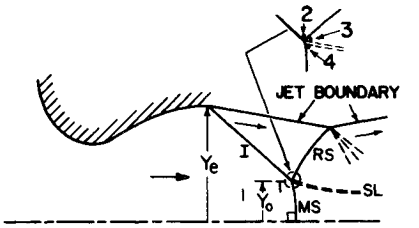

Fig. 1 Mach reflection from two-dimensional over-expanded nozzle flow.

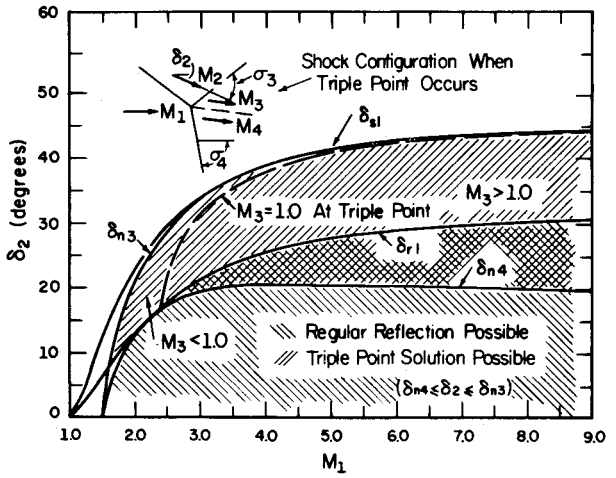

Fig. 2 Flow regimes of two-dimensional nozzle-free jet flow according to incident shock strength.

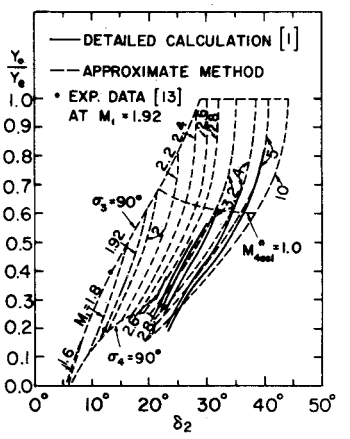

Fig. 4 Two-dimensional Mach stem height corresponding to incident shock strength.

results of the interaction between the outer and central core streams downstream of the triple point. It is expected that the occurrence of the Mach reflection and the subsequent interaction between the streams should be such that an equivalent "choking" condition prevails for the downstream central core flow. Indeed, this type of consideration has been adopted for the study of supersonic ejector systems[4] and for the calculations of Mach disk for overexpanded[5] and under-expanded axisymmetric nozzle flows.[6-8] In all these later calculations, the slower central core flow was approximated by a simple one-dimensional analysis so that the "choking" condition can be interpreted as "sonic flow at a section of minimum area." It was also pointed out for two-dimensional flow problems[9] that the interaction between the outer stream, and the central core flow is such that the one-dimensional description for the latter cannot be employed to match the former in the early portion of the flow development. A single strip analysis based on the "method of integral relations"[10] was thus employed to study this early flow development. Extensive calculations have been carried out and meaningful results have been obtained. A portion of the results has been reported[9] as samples of calculations. Detailed procedures of calculations are already reported[1] and will not be repeated here. For the benefit of discussion, some of the results are shown in Figs. 2–4. Figure 2 identifies various flow regimes

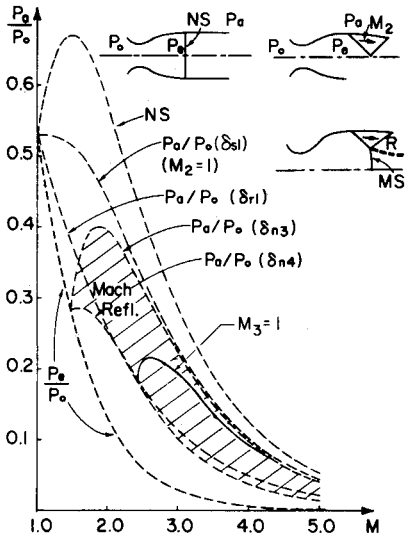

Fig. 3 Corresponding back pressure ratio for two-dimensional nozzle free jet flow.

pertaining to the incident shock strength (given by M_1 and the absolute value of δ_2) for two-dimensional flow situations. Since Mach reflection must be associated with the appearance of a triple point, it may readily be concluded that Mach reflection can only occur for $\delta_{n4} \leq \delta_2 \leq \delta_{n3}$ where δ_{n3} and δ_{n4} are values of δ_2 such that the reflected and Mach shock are normal shocks, respectively, at the triple point. The curve dividing the subsonic and supersonic states behind the reflected shock ($M_3 = 1$) at the triple point is also identified. Figure 3 shows the corresponding pressure ratio for these flow regimes which can obviously be determined when M_1 and δ_2 are known. For reference purposes, the isentropic pressure ratio of the nozzle and the back pressure ratio corresponding to the condition of a normal shock occurring at the exit section of the nozzle are also plotted in the same figure. Figure 4 presents the established Mach stem height by detailed interaction calculations when the state behind the reflected shock is supersonic at the triple point ($M_3 > 1$ in Fig. 2). This is possible only if the nozzle Mach number is larger than 2.406 (for $\gamma = 1.4$) according to Fig. 2. These results are plotted in solid lines in Fig. 4 whose upper limits are imposed by the condition of $M_3 = 1$ at the triple point.

For higher pressure ratios or smaller nozzle Mach numbers ($M_1 < 2.406$), the state behind the reflected shock is subsonic at the triple point, and such detailed calculations by marching downstream from the triple point are not possible. It is known[11,12] that for subsonic corner flow behind the shock attached to a finite wedge, infinite shock curvature generally occurs at the tip, and the viscous effects are thus becoming important. It is anticipated that similar behavior would prevail under the present flow situations. Indeed, detailed inviscid interactive calculations by the method of integral relations[1] immediately behind the triple point have not been able to yield any meaningful results. However, it is the intention of this paper to show that despite the trouble encountered in the establishment of the detailed flow pattern under these flow conditions, it is still possible to estimate the location and size of the Mach stem by paying particular attention to the interacting force between the streams. The method of analysis is simple and results obtained are quite reasonable in comparison with the available experimental data. In addition, this approximate method has also produced comparable results where detailed inviscid interactive calculations of the flowfield are possible ($M_3 > 1$).

Perhaps it should be mentioned that for cases with relatively large nozzle Mach numbers, the flow would have been separated away from the wall under this highly over-expanded flow condition and Mach reflection with a nonuniform approaching flow prevails. This complicated flow pattern cannot be hopefully studied before the corresponding Mach reflection pattern with uniform approach flow has been successfully analyzed. As an initial step, it is entirely logical to ignore completely the viscous

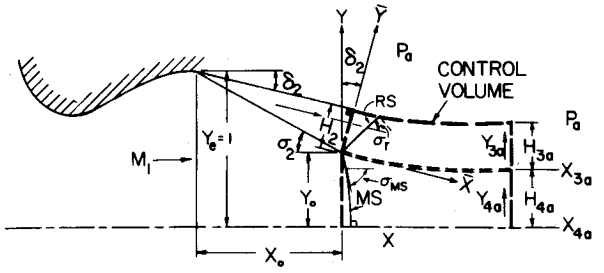

Fig. 5 Two-dimensional nozzle free jet flow with Mach reflection at high back pressure.

effects occurring along the nozzle wall, the jet boundary as well as the slipline between the streams.

Theoretical Considerations

Two-Dimensional Flow

It should be recognized that under the flow condition when subsonic states occur behind the reflected shock wave at the triple point ($M_3 < 1$), the strength of the reflected shock is not truly strong even when it belongs to the strong shock branch, as the state behind the incident wave (state 2) is not far away from sonic condition. It is also expected that the reflected shock strength is reduced quickly as it proceeds away from the triple point. It would be quite convenient to assume that it degenerates into a Mach wave when it intersects with the free jet boundary. This assumption is in contrast with the usual expectation[13] that the sonic line shall originate at the intersection with the free jet boundary. It is expected, however, that this difference in the estimation of dissipation is very small.

In referring to Fig. 5, where such a two-dimensional flow is depicted, one may write for the reflected shock according to the assumption previously described that

$$\sigma_r(\bar{Y}) = \alpha_2 + (\sigma_3 - \alpha_2)[1 - (\bar{Y}/H_2)]^2 \tag{1}$$

where σ_r is the wave angle of the curved reflected shock, σ_3 is its value at the triple point, and α_2 is the Mach angle of the fluid state 2. Similarly, one may also estimate the Mach shock shape MS as given by

$$\sigma_{MS}(Y) = \sigma_4 + [-(\pi/2) - \sigma_4][1 - (Y/Y_o)]^2 \tag{2}$$

where σ_{MS} is the wave angle of the Mach shock and σ_4 is that at the triple point. It is then stipulated that no additional dissipation incurred within the downstream flowfield. The flow will subsequently expand and assume the final asymptotic rotational state corresponding to the ambient pressure p_a at far downstream positions. Such a stipulation does not seem to be unreasonable. Since under these flow conditions within this flow regime, even if additional shocks appear in the downstream flowfield, they are relatively weak and the incurred loss would be negligible.

One realizes from the continuity principle for elementary stream tube that

$$\rho_{3a} V_{3a}\, dY_{3a} = \rho_2 V_2\, d\bar{Y} \tag{3}$$

and

$$\rho_{4a} V_{4a}\, dY_{4a} = \rho_1 V_1\, dY \tag{4}$$

Upon introducing normalizational factors and realizing that isentropic process prevails along stream tubes, H_{3a} and H_{4a} can be obtained readily from

$$H_{3a} = \int dY_{3a} = \frac{V_2}{V_m}\int_o^{H_2}\left(\frac{p_{o2}}{p_{o3a}}\right)^{(\gamma-1)/\gamma}\cdot\frac{V_m}{V_{3a}}\,d\bar{Y} \tag{5}$$

and

$$H_{4a} = \int dY_{4a} = \frac{V_1}{V_m}\left(\frac{p_1}{p_a}\right)^{1/\gamma}\int_o^{Y_o}\left(\frac{p_{o1}}{p_{o4a}}\right)^{(\gamma-1)/\gamma}\cdot\frac{V_m}{V_{4a}}\,dY \tag{6}$$

where

$$\frac{V_{3a}}{V_m} = \left[1 - \left(\frac{p_a}{p_{o1}}\frac{p_{o1}}{p_{o2}}\frac{p_{o2}}{p_{o3a}}\right)^{(\gamma-1)/\gamma}\right]^{1/2} \tag{7a}$$

$$\frac{V_{4a}}{V_m} = \left[1 - \left(\frac{p_a}{p_{o1}}\frac{p_{o1}}{p_{o4a}}\right)^{(\gamma-1)/\gamma}\right]^{1/2} \tag{7b}$$

and the stagnation pressure ratios p_{o3a}/p_{o2} and p_{o4a}/p_{o1} represent the loss incurred from the reflected and Mach shock, respectively. They may be evaluated readily when the wave angles σ_r, σ_{MS} are given by Eqs. (1) and (2).

Application of the momentum principle in the main direction of flow associated with the control volume as shown in Fig. 5 would yield

$$Y_o\left[\frac{p_1}{p_{o1}}(1+\gamma M_1^2) - \frac{p_a}{p_{o1}}\right] = \frac{2\gamma}{\gamma-1}\left(\frac{p_a}{p_{o1}}\right)^{1/\gamma}\left[\left(\frac{p_{o2}}{p_{o1}}\right)^{(\gamma-1)/\gamma}\times\right.$$
$$\int_o^{H_{3a}}\left(\frac{p_{o3a}}{p_{o2}}\right)^{(\gamma-1)/\gamma}\left(\frac{V_{3a}}{V_m}\right)^2 dY_{3a} + \int_o^{H_{4a}}\left(\frac{p_{o4a}}{p_{o1}}\right)^{(\gamma-1)/\gamma}\times$$
$$\left.\left(\frac{V_{4a}}{V_m}\right)^2 dY_{4a} - \left(\frac{p_{o2}}{p_{o1}}\right)^{(\gamma-1)/\gamma}\left(\frac{V_2}{V_m}\right)^2 H_2\cos\delta_2\right] \tag{8}$$

In addition, the geometrical configuration gives

$$H_2 = (1 - Y_o + X_o\tan\delta_2)\cos\delta_2 \tag{9}$$

where

$$X_o = -(1 - Y_o)/\tan\sigma_2 \tag{10}$$

For a particular nozzle Mach number M_1 at a certain ambient pressure ratio p_a/p_{o1} such that Mach reflection pattern prevails, values of H_{3a}, H_{4a}, and Y_o are unknown, and they may be solved from Eqs. (5, 6, and 8) through iterative procedures. With the given M_1 and the pressure ratio p_a/p_{o1}, state 2 behind the incident shock can be determined from the oblique shock relations. States 3 and 4 and the wave configuration at the triple point can also be uniquely found from the conditions that states 3 and 4 shall have the same pressure and flow direction. With a selected value of Y_o as the Mach stem height, it is obvious that X_o and H_2 can be obtained from Eqs. (9) and (10) while H_{3a} and H_{4a} can be found from Eqs. (5) and (6) by integrations. The correct value of Y_o would finally satisfy Eq. (8). The method of false position was found to be extremely efficient for this purpose and final results are obtained in few iterations even for widely different initial values of Y_o. The results obtained from these calculations are also presented in Fig. 4 (identified by dashed lines). For reference purposes, the states when the fluid immediately below the slipline reaches sonic asymptotic condition are also identified in the same figure.

Axisymmetric Flows

Previous calculations of the axisymmetric flowfield within the over-expanded flow regime[5] were restricted only for supersonic state behind the reflected shock ($M_3 > 1$). It is obvious that this approximate method for two-dimensional problems can be extended to axisymmetric flows. It should be recognized that under this flow condition, the incident shock is no longer

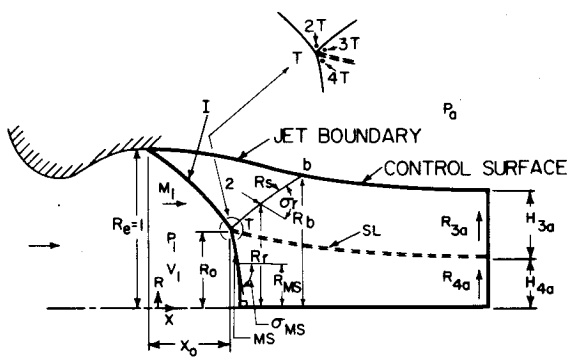

Fig. 6 Axisymmetric flowfield with Mach reflection at high back pressure.

straight, and the flow between the incident and the reflected shock is nonuniform. A step-by-step build-up of the flowfield by the rotational method of characteristics is necessary before the calculations of the triple point, and the subsequent interacting flowfield by the present approximate method can be implemented. Referring to Fig. 6, a parabolic variation is assumed again for the reflected shock wave angle which may be written as

$$\sigma_r = \alpha_b + (\sigma_{3_T} - \alpha_b)\left(1 - \frac{R_r - R_o}{R_b - R_o}\right)^2 \tag{11}$$

where σ_{3_T} is the reflected shock wave angle at the triple point state 3_T.

It is also convenient to express the shape of the reflected shock by

$$R_r = ax^2 + bx + c \tag{12}$$

where $a = \tan(\alpha_b + \theta_b) - \tan(\sigma_{3_T} + \delta_{2_T})$; $b = \tan(\sigma_{3_T} + \delta_{2_T}) - 2aX_o$; and $c = R_o - aX_o^2 - bX_o$, which can only be determined after the method of characteristics has been applied to calculate the flow behind the incident shock and the triple point location has been established. Similarly, for the wave angle of the Mach shock, one may write again

$$\sigma_{MS} = \sigma_{4_T} + [-(\pi/2) - \sigma_{4_T}][1 - (R_{MS}/R_o)]^2 \tag{13}$$

where σ_{4_T} is its value at the triple point state 4_T.

One may also obtain from continuity principle

$$\frac{H_{4a}^2}{2} = \left(\frac{p_1}{p_a}\right)^{1/\gamma}\left[1 - \left(\frac{p_1}{p_{o1}}\right)^{(\gamma-1)/\gamma}\right]^{1/2} \times \int_o^{R_o}\left(\frac{p_{o1}}{p_{o4a}}\right)^{(\gamma-1)/\gamma} R_{MS}\, dR_{MS} \Big/ \left[1 - \left(\frac{p_a}{p_{o1}}\frac{p_{o1}}{p_{o4a}}\right)^{(\gamma-1)/\gamma}\right]^{1/2} \tag{14}$$

and

$$\left(\frac{H_{3a}}{2} + H_{4a}\right)H_{3a} = \left(\frac{p_1}{p_a}\right)^{1/\gamma}\left[1 - \left(\frac{p_1}{p_{o1}}\right)^{(\gamma-1)/\gamma}\right]^{1/2} \times \int_{R_o}^{1}\left(\frac{p_{o1}}{p_{o3a}}\right)^{(\gamma-1)/\gamma} R\, dR \Big/ \left[1 - \left(\frac{p_a}{p_{o1}}\frac{p_{o1}}{p_{o3a}}\right)^{(\gamma-1)/\gamma}\right]^{1/2} \tag{15}$$

where the stagnation pressure ratio p_{o4a}/p_{o1} and p_{o3a}/p_{o1} are associated with the losses due to the Mach shock and incident-reflected shock system, respectively. The momentum relationship applied to the control volume as shown in Fig. 6 would yield

$$\frac{p_1}{p_{o1}}(1+\gamma M_1^2) - \frac{p_a}{p_{o1}} = \frac{4\gamma}{\gamma-1}\left(\frac{p_a}{p_{o1}}\right)^{1/\gamma}\left[\int_o^{H_{4a}}\left(\frac{p_{o4a}}{p_{o1}}\right)^{(\gamma-1)/\gamma} \times \left(\frac{V_{4a}}{V_m}\right)^2 R\, dR + \int_o^{H_{3a}}\left(\frac{p_{o3a}}{p_{o1}}\right)^{(\gamma-1)/\gamma}\left(\frac{V_{3a}}{V_m}\right)^2 (H_{4a}+R)\, dR\right] \tag{16}$$

For each particular flow condition, calculation by the method of characteristics must be carried out until the triple point condition can be satisfied on the incident shock. The precise location of the triple point corresponding to the pressure ratio is again determined through iteration procedures until Eq. (16) is satisfied. The results of these calculations are presented in Fig. 7.

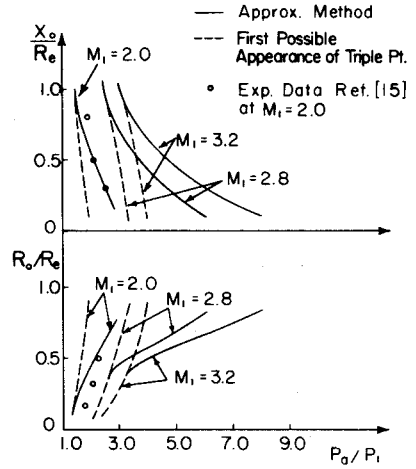

Fig. 7 Size and location of Mach disk for over-expanded axisymmetric nozzle flow.

Discussion

From the results obtained for two-dimensional and axisymmetrical flows, it is indeed interesting to observe the trend and change in the flow as influenced by the ambient pressure ratio within this over-expanded flow regime. A limited amount of experimental data from Ferri[14] and Love et al.[15] are also plotted for comparison purposes. The agreement is fairly reasonable in view of the fact that the viscous effects tend to modify the inviscid results significantly within this flow regime. It should be emphasized here that the presented method, stressing the mutual interacting force between the two streams, was originally developed to deal with situations with subsonic flow behind reflected shocks at the triple point. It is of course surprising to find that it has also yielded comparable results where the detailed inviscid calculations of the flowfield are possible.

It should be pointed out that it is not clear how the flow pattern changes from the regular reflection regime to the Mach reflection regime as the ambient pressure ratio is increased. The situation of $\sigma_4 = 90°$ at the triple point probably would never be realized since the outer stream is then undergoing a regular reflection. Perhaps the study of the flowfield associated with regular reflection but with strong curved reflected shock could explain the sequence of events between these regimes. On the other hand, one observes from Fig. 4 that for a smaller nozzle Mach number, there is a maximum Mach stem height that may appear from these calculations. Although this maximum value may be related to the specific assumption adopted for the analysis and thus may be different for different assumptions (e.g., immediate decay of the reflected shock into a Mach wave at the triple point would have resulted in longer Mach stems), it will not reach the height of the nozzle since the reflected shock is approaching a normal shock at the triple point. Because the state behind the incident wave is not far from sonic flow under these conditions, normal shock becomes, in reality, a Mach wave, and this Mach reflection regime would merge smoothly into the strong curved shock regime. It is obvious from Fig. 3 that there is a wide range of the ambient pressure ratio for various nozzle Mach numbers corresponding to this strong curved shock regime. Preliminary investigation of the flow within this regime has indicated that this particular type of problem exhibits specific behavior which typically exemplifies the elliptic character of the flow, and the generated vorticity seems to play an important role in the solution of these flow problems.

References

[1] Chang, I. S., "Mach Reflection, Mach Disc, and the Associated Nozzle Free Jet Flows," Ph.D. thesis, 1973, Dept. of Mechanical and Industrial Engineering, University of Illinois at Urbana-Champaign, Urbana, Ill.; available from University MicroFilm Service, Ann Arbor, Mich., Micro No. 74-11973.

[2] Bleakney, W. and Taub, A. H., "Interaction of Shock Waves," *Reviews of Modern Physics*, Vol. 21, 1949, pp. 584–605.

[3] Polacheck, H. and Seeger, R. J., "Shock Wave Interactions," Sec. E., *Fundamentals of Gas Dynamics*, Vol. III of High Speed Aerodynamics and Jet Propulsion, Princeton University Press, Princeton, N.J., 1958.

[4] Chow, W. L. and Addy, A. L., "Interaction between Primary and Secondary Streams of Supersonic Ejector Systems and their Performance Characteristics," *AIAA Journal*, Vol. 2, April 1964, p. 686.

[5] Ashratov, E. A., "Calculations of Axisymmetric Jet Leaving a Nozzle at Jet Pressure Lower than Pressure in Medium," *Fluid Dynamics* (translated from Russian), Vol. 1, 1966, p. 113.

[6] Abbett, M., "Mach Disk in Underexpanded Exhaust Plumes," *AIAA Journal*, Vol. 9, March 1971, pp. 512–514.

[7] Fox, J. H., "On the Structure of Jet Plumes," *AIAA Journal*, Vol. 12, Jan. 1974, pp. 105–107.
[8] Chang, I. S. and Chow, W. L., "Mach Disc from Underexpanded Axisymmetric Nozzle Flow," *AIAA Journal*, Vol. 12, Aug. 1974, pp. 1079–1082.
[9] Chow, W. L. and Chang, I. S., "Mach Reflection from Overexpanded Nozzle Flows," *AIAA Journal*, Vol. 10, Sept. 1972, pp. 1261–1263.
[10] Traugott, S. C., "An Approximate Solution of the Direct Supersonic Blunt Body Problem for Arbitrary Axisymmetric Shapes," *Journal of the Aerospace Science*, Vol. 27, May 1960, pp. 361–370.
[11] Buseman, A., "A Review of Analytical Methods for the Treatment of Flows with Detached Shocks," TN 1858, 1949, NACA.
[12] Sternberg, J., "Triple-Shock-Wave Interactions," *The Physics of Fluids*, Vol. 2, Feb. 1959, pp. 179–206.
[13] Guderley, K. G., *The Theory of Transonic Flow*, Pergamon, Addison-Wesley, Reading, Mass., 1962, pp. 144–149.
[14] Ferri, A., *Elements of Aerodynamics of Supersonic Flows*, Macmillan, New York, 1949, pp. 177.
[15] Love, E. S. and Grigsby, C. E., "Some Studies of Axisymmetric Free Jets Exhausting from Sonic and Supersonic Nozzles into Still Air and into Supersonic Streams," RM L43L31, May 1958, NACA.

JUNE 1975 AIAA JOURNAL VOL. 13, NO. 6

Hydrodynamic Stability of the Far Wake of a Hovering Rotor

BHARAT P. GUPTA*
Bell Helicopter Co., Fort Worth, Texas
AND
MARTIN LESSEN†
University of Rochester, Rochester, N.Y.

The stability of a continuous model for the far wake of a hovering rotor has been formulated and analyzed. In the continuous model representation of the far wake, the vorticity of the interdigitated circular vortex helices is assumed to be distributed over a vortex sheet, and the potential flow inside and outside of the vortex sheet is taken to correspond to the average velocity profiles calculated for an interdigitated representation. A continuum of instabilities is found to exist for all wave numbers and for all modes except in some specific situations where the flow is neutrally stable. This model gives the instabilities of the gross flow and complements the interdigitated analysis of Ref. 1 which is the companion analysis for the instabilities of centerline displacements of the vortex helices.

Introduction

A STABILITY analysis of an interdigitated trailing vortex model of a hovering rotor for centerline displacement type of perturbations has been carried out by Gupta and Loewy.[1] The stability of the gross flow in the far wake of a hovering rotor, however, may be studied in a manner similar to that used by Lessen et al.[2] and by Uberoi[3] in their studies of trailing line vortices and jets.

By far wake, we mean the portion of the wake which is influenced by the vortex elements approximately one helix revolution away from the rotor, and where the induced effects of the lifting line vortex representation are insignificant. The reason for restricting the analysis to the far wake is that in the near wake, the lifting line has a stabilizing effect and therefore the near wake is expected to be more stable than the far wake. The relative stability of the near wake has been demonstrated by experimental rotor wake visualization studies and by theoretical free wake analyses where distortions of the wake due to induced velocities are considered.

Received May 20, 1974; revision received December 6, 1974.
Index category: Rotary Wing Aerodynamics.

* Research Engineer, Aeroacoustics; formerly a graduate student in the Department of Mechanical and Aerospace Sciences, University of Rochester, Rochester, N.Y.
† Professor, Department of Mechanical and Aerospace Sciences.

The far wake stability problem is important for several reasons, the most important one being the persistence of the wake of a hovering rotorcraft in the atmosphere and the pitching moments experienced by another aircraft flying into this wake. In such situations one might be interested to know the modal instabilities of the wake to arbitrarily small perturbations introduced by atmospheric disturbances and turbulence.

Another important reason concerns the numerical stability of the free wake type of analyses which are frequently used and which are found to be unsatisfactory in most hovering situations.

Finally, viscosity effects in the following analysis have been neglected because of the high Reynolds number associated with the flows. Reynolds numbers associated with the flows are of the order of 10^5–10^7 in most practical operating situations, and stability analyses of jets and wakes have indicated that viscous damping effects are negligible for Reynolds numbers greater than 50. In addition, it has been found that "top-hat" velocity and vorticity distributions, as representing actual jet and vortex combinations, have yielded stability results in good agreement with calculations of more accurate flowfield representations.

Velocity Profiles in the Far Wake

The far wake of a hovering helicopter can be represented by doubly infinite circular concentric helical vortices trailing from the root and tip of each blade. The details of induced velocity